

Bipodal Surface Organometallic Complexes with Surface N-Donor Ligands and Application to the Catalytic Cleavage of C–H and C–C Bonds in *n*-Butane

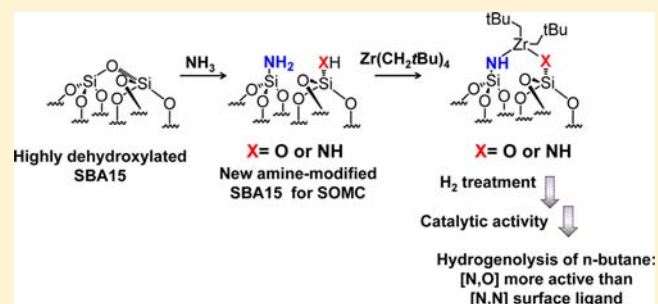
Anissa Bendjeriou-Sedjerari,[†] Joachim M. Azzi,[†] Edy Abou-Hamad,[†] Dalaver H. Anjum,[†] Fahran A. Pasha,[†] Kuo-Wei Huang,[†] Lyndon Emsley,[‡] and Jean-Marie Basset^{*,†}

[†]KAUST Catalysis Center (KCC), King Abdullah University of Science & Technology, 23955-6900 Thuwal, Saudi Arabia

[‡]Université de Lyon, Institut de Sciences Analytiques (CNRS, ENS-Lyon, UCB Lyon 1), Centre de RMN à Très Hauts Champs, 5 rue de la Doua, 69100 Villeurbanne, France

Supporting Information

ABSTRACT: We present a new generation of “true vicinal” functions well-distributed on the inner surface of SBA15: [(≡Si–NH₂)(≡Si–OH)] (1) and [(≡Si–NH₂)₂] (2). From these amine-modified SBA15s, two new well-defined surface organometallic species [(≡Si–NH–)(≡Si–O–)]Zr(CH₂tBu)₂ (3) and [(≡Si–NH–)₂]Zr(CH₂tBu)₂ (4) have been obtained by reaction with Zr(CH₂tBu)₄. The surfaces were characterized with 2D multiple-quantum ¹H–¹H NMR and infrared spectroscopies. Energy-filtered transmission electron microscopy (EFTEM), mass balance, and elemental analysis unambiguously proved that Zr(CH₂tBu)₄ reacts with these vicinal amine-modified surfaces to give mainly bipodal bis(neopentyl)zirconium complexes (3) and (4), uniformly distributed in the channels of SBA15. (3) and (4) react with hydrogen to give the homologous hydrides (5) and (6). Hydrogenolysis of *n*-butane catalyzed by these hydrides was carried out at low temperature (100 °C) and low pressure (1 atm). While (6) exhibits a bis(silylamido)zirconium bishydride, [(≡Si–NH–)₂]Zr(H)₂ (6a) (60%), and a bis(silylamido)-silyloxozirconium monohydride, [(≡Si–NH–)₂(≡Si–O–)]ZrH (6b) (40%), (5) displays a new surface organometallic complex characterized by an ¹H NMR signal at 14.46 ppm. The latter is assigned to a (silylimido)(silyloxo)zirconium monohydride, [(≡Si–N=)(≡Si–O–)]ZrH (5b) (30%), coexistent with a (silylamido)(silyloxo)zirconium bishydride, [(≡Si–NH–)(≡Si–O–)]Zr(H)₂ (5a) (45%), and a silylamidobis(silyloxo)zirconium monohydride, [(≡Si–NH–)(≡Si–O–)₂]ZrH (5c) (25%). Surprisingly, nitrogen surface ligands possess catalytic properties already encountered with silicon oxide surfaces, but interestingly, catalyst (5) with chelating [N,O] shows better activity than (6) with chelating [N,N].



INTRODUCTION

Surface organometallic chemistry (SOMC), the interface between homogeneous and heterogeneous catalysis, can construct relatively well-defined active sites with the main objective of the rational design of catalysis. SOMC has provided insight in areas such as alkane and olefin metathesis, hydrogenolysis of polyolefins, the activation of dinitrogen, etc.^{1–18} Understanding the reactions of organometallic complexes with several metal oxide supports has enabled the preparation of a series of “single site” catalysts on well-defined surfaces with several key advantages, such as the ability to follow the in situ, in operando behavior of surface organometallic complexes at high temperatures. A range of oxide supports such as zeolite,^{19,20} silica,³ silica–alumina,²¹ alumina,²² niobia,²³ titania,²⁴ and mesoporous materials (SBA15, MCM41)^{25–27} have been employed, and many elements of the periodic table have been grafted onto those supports.¹ However, while significant progress in SOMC has been made in the last two decades, these systems rely on creating one to

several well-defined σ or π bonds between transition metal elements and metal oxide surfaces. The options to control the catalyst properties are thus limited, and the further development and improvement of surface organometallic systems is currently restricted.

Amido ligands have emerged as extremely versatile tools for ligand design in the field of coordination chemistry.^{28–34} Complexes with ligands containing coordinating nitrogen atoms can sometimes provide improved catalytic activity with respect to their oxygenated counterparts.³⁵ From group 3 to group 12, a whole range of transition metal complexes involving a variety of nitrogen ligands have been fully documented and extended to lanthanides.^{36–47} Many such complexes have demonstrated potential activities toward olefin polymerization,^{48–52} ring-opening polymerization (ROP),⁵³ synthesis of ammonia,⁵⁴ metathesis,^{55–59} and C–H activation.^{60–63} For

Received: September 5, 2013

Published: November 6, 2013

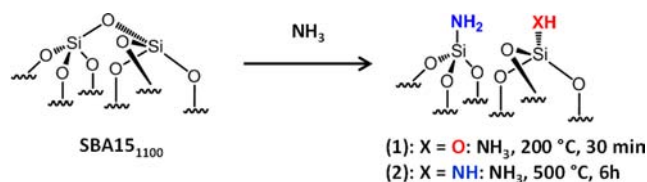
example, the catalytic cleavage of C–H/C–C bonds in higher alkanes (paraffins) is still a considerable challenge. Their transformation into lower alkanes is a highly temperature- and energy-intensive process. If such reactions could be carried out faster at much lower temperature, it would be an economic and environmental breakthrough. Catalytic hydrogenolysis of several simple alkanes by metal hydrides supported on silica at mild temperature is well-documented.^{64–71} Nevertheless, in molecular chemistry, group 4 d⁰ organometallic molecules with alkoxide or siloxide ligands have demonstrated very little reactivity, despite their apparent electronic unsaturation. In contrast, the same systems bearing bulky silylamido ligands have shown C–H activation via transient putative imido complexes [(*t*Bu₃SiNH)₂M=NSi(*t*Bu₃)].^{72–81}

Access to silica surfaces bearing amine functionalities is known to be possible through ammonia treatment of silica at different temperatures and flow rates.^{82–91} Nonetheless, to our knowledge there have been no previous reports of amine-modified surface organometallic chemistry. To address the limitations described above, in this work we developed a new generation of surface organometallic complexes with either nitrogen or mixed nitrogen/oxygen surface ligands. Thus, novel designs of heterogeneous zirconium hydride complexes with at least one silylamido ligand directly connected to the surface are presented. These new amine-modified surface organometallic complexes are good candidates to elucidate fundamental understanding of the different events that govern C–H activation.

RESULTS AND DISCUSSION

Generation of Well-Defined Silylamine/Silanol and Bis-Silylamine Pairs on SBA15₁₁₀₀ Surfaces. SBA15, one of the most attractive host materials, was chosen as an oxide support because of its high surface area, large uniform pore diameter (6 nm), thicker walls (3 to 6 nm), and high thermal stability (up to 1473 K).^{92,93} Two kinds of amine-modified SBA15 materials bearing either silylamine/silanol pairs, (1), or bis-silylamine pairs, (2), were obtained by ammonia treatment of highly dehydroxylated SBA15 prepared at 1100 °C (SBA15₁₁₀₀). This support is well-known to contain mainly strained reactive siloxane bridges (≡Si–O–Si≡) that result from the condensation of silanols (adjacent and geminal) along with a small amount of isolated silanols remaining on the surface.^{91,94} The silicon atom in a strained siloxane bridge is electron-deficient. Acting as a Lewis acid, it is therefore highly reactive toward ammonia.^{84,85,88–91,95} As described in Scheme 1, chemisorption of ammonia at 200 °C for 30 min leads primarily to opening of these siloxane bridges to generate silanol/silylamine pairs (1). A longer thermal treatment at higher temperature (500 °C, 6 h) results in the substitution of

Scheme 1. Synthesis of Paired Silylamine/Silanol [(≡Si–NH₂)(≡Si–OH)] (1) and Paired Bis-Silylamine [(≡Si–NH₂)₂] (2) by Controlled Treatment with Ammonia



the silanols previously formed to generate bis-silylamine pairs (2).

The infrared spectrum of SBA15₁₁₀₀ contains the characteristic $\nu_s(\text{OH})$ band of single silanol groups at 3748 cm⁻¹ (Figure 1i).⁹¹ After ammonia treatment at 200 °C for 30 min, an

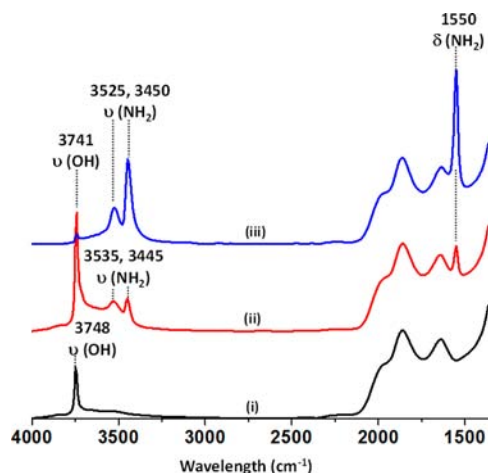


Figure 1. IR spectra of SBA15₁₁₀₀ (i) before NH₃ treatment, (ii) after NH₃ treatment at 200 °C for 30 min to give (1), and (iii) after NH₃ treatment at 500 °C for 6 h to give (2).

increase in intensity of this band is observed with a red shift from 3748 to 3741 cm⁻¹.⁸⁹ Additionally, three new vibration bands appear at 3535, 3445, and 1550 cm⁻¹ corresponding to the $\nu_s(\text{NH}_2)$, $\nu_{as}(\text{NH}_2)$, and $\delta(\text{NH}_2)$ bands, respectively (Figure 1ii). In both cases, IR bands characteristic of physisorbed ammonia do not appear at 3380, 3290, and 1608 cm⁻¹, which would correspond to the stretching vibration and deformation bands of the N–H bond.⁸² The IR spectrum of (2) shows almost complete disappearance of stretching vibration bands at 3748 and 3741 cm⁻¹ and bands characteristic of $\nu(\text{NH}_2)$ appear with a shift to lower wavelength at 3525 and 3450 cm⁻¹ (Figure 1iii). The $\delta(\text{NH}_2)$ band appears at 1550 cm⁻¹. All of these IR results indicate chemisorption of ammonia, but they do not confirm the concept of adjacent silanol/silylamine or bis-silylamine functionalities.

For this purpose, both materials were fully characterized by solid-state NMR spectroscopy. The ¹H magic-angle-spinning (MAS) spectrum of (1) displays a strong signal at 0.61 ppm assigned to the silylamine, ≡SiNH₂ (Figure 2a).^{83,96} The second resonance observed at 1.73 ppm corresponds to both the isolated silanols, ≡SiOH, and the new silanols formed by ammonia treatment. Regarding the ¹H MAS spectrum of (2), only one resonance is observed at 0.64 ppm, corresponding to the silylamine species (Figure 2b). These results are a further proof of complete chemisorption of ammonia (no silanols persist in 2). The proton chemical shift of ammonia physisorbed on silica would appear at 2.4 ppm.⁵

To characterize the presence of vicinal silylamine/silanol (1) as well as bis-silylamine pairs (2) on the SBA15 surfaces, 2D multiple-quantum (MQ) proton NMR experiments were performed. The double-quantum (DQ) spectra of both materials show strong autocorrelation peaks on the 2:1 diagonal centered at around 0.6 ppm in F2 and 1.2 ppm in F1 (Figure 2c,d). This resonance is assigned to the ≡SiNH₂ moiety. It confirms that at least two equivalent protons are present on the grafted nitrogen in both species. In the DQ spectrum in Figure

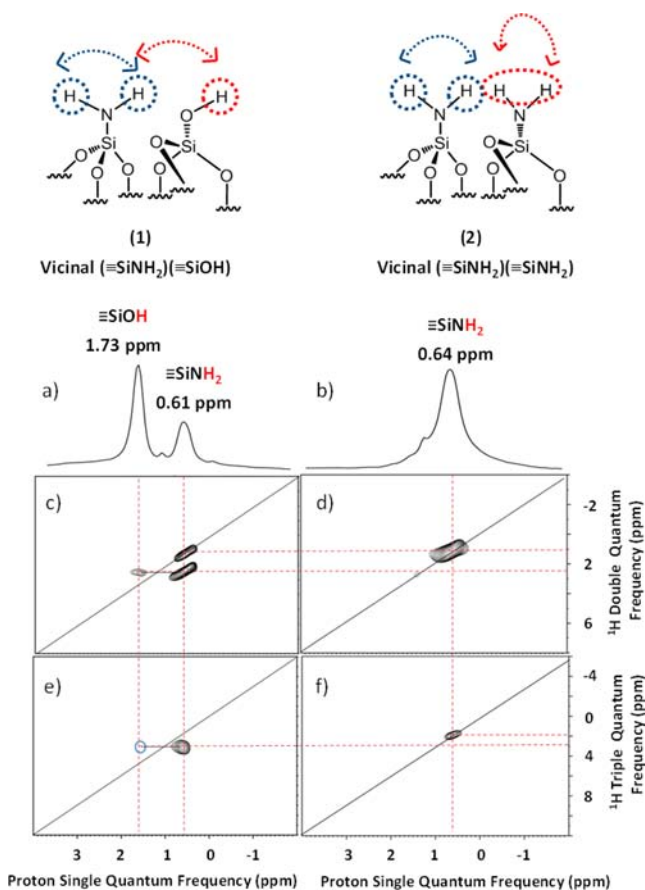


Figure 2. (a, b) ^1H MAS NMR spectra of (1) and (2), respectively. (c, d) DQ rotor-synchronized 2D ^1H MAS spectra of (1) and (2), respectively. (e, f) ^1H TQ MAS spectra of (1) and (2), respectively.

2c, the proton resonance assigned to $\equiv\text{SiNH}_2$ at 0.6 ppm shows a strong correlation with the proton at 1.7 ppm assigned to $\equiv\text{SiOH}$ [2.3 ppm in F1: $\delta_{\text{H}}(\text{NH}_2) + \delta_{\text{H}}(\text{OH}) = 0.6 + 1.7$]. In other words, this corresponds to the correlation between $\equiv\text{SiNH}_2$ and $\equiv\text{SiOH}$ protons in close proximity (typically <5 Å). Thus, the silanol/silylamine pairs detected in IR are in very close proximity in (1), as expected from our strategy. Moreover, the correlation between one proton from one $\equiv\text{SiNH}_2$ and the two protons from the neighboring silylamine in (2) is highlighted in the ^1H triple-quantum (TQ) solid-state NMR spectrum of Figure 2f. Thus, the ^1H TQ chemical shift of $\equiv\text{SiNH}_2$ species appears at 1.92 ppm [$3\delta_{\text{H}}(\text{NH}_2)$]. This correlation shows that the two silylamine groups are in close proximity in (2). The ^1H TQ solid-state NMR spectrum of (1) was also recorded (Figure 2e). It shows a correlation at about 3 ppm corresponding to [$2\delta_{\text{H}}(\text{NH}_2) + \delta_{\text{H}}(\text{OH}) = 2 \times 0.6 + 1.73$], which is again consistent with the proposed structure.

Reactivity of $\text{Zr}(\text{CH}_2\text{tBu})_4$ with $[(\equiv\text{Si}-\text{NH}_2)(\equiv\text{SiOH})]$, (1) and $[(\equiv\text{Si}-\text{NH}_2)_2]$, (2). The reactions of $\text{Zr}(\text{CH}_2\text{tBu})_4$ with (1) and (2) were conducted by an impregnation method in *n*-pentane to yield $[(\equiv\text{Si}-\text{NH})(\equiv\text{Si}-\text{O})]\text{Zr}(\text{CH}_2\text{tBu})_2$ (3) and $[(\equiv\text{Si}-\text{NH})_2]\text{Zr}(\text{CH}_2\text{tBu})_2$ (4), respectively (Scheme 2).⁹⁷

The IR spectra of these materials obtained after reaction are quite similar (Figures 3 and 4). As expected, a strong decrease in the intensity of the NH_2 and OH vibrational and stretching bands is observed. New bands at 3208 and 3350 cm^{-1} are assigned to the $\nu(\text{NH})$ vibration.^{17,78,98,99} Vibrational bands of

Scheme 2. Reaction of $\text{Zr}(\text{CH}_2\text{tBu})_4$ with (1) and (2) in Dry *n*-Pentane at RT for 8 h

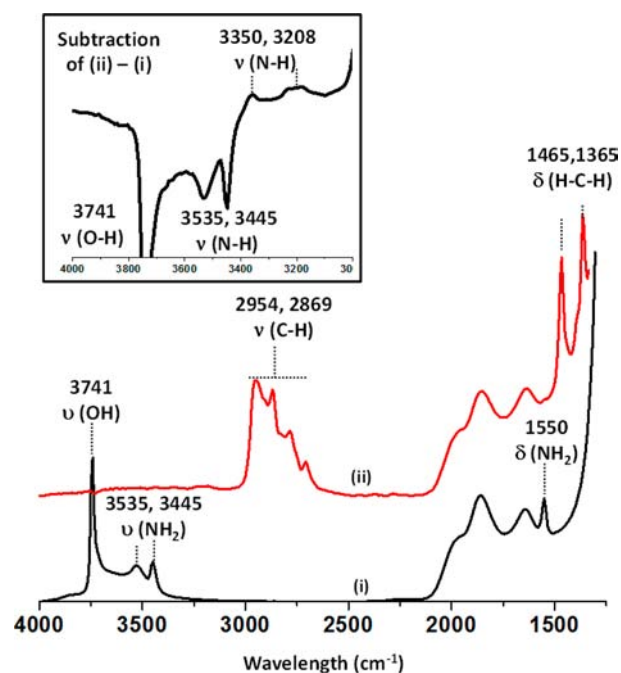
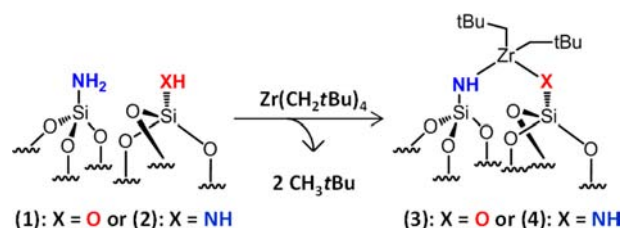


Figure 3. IR spectra of (1) (i) before and (ii) after reaction with $\text{Zr}(\text{CH}_2\text{tBu})_4$ to give (3). Inset: difference spectrum [(ii) - (i)] showing the disappearance of the ($\equiv\text{SiNH}_2$) stretch modes (3445 and 3535 cm^{-1}) and the appearance of the (μ -(NH)Si(=))(OSi(=)) bending mode.

neopentyl moieties appear at 2954 [$\nu_{\text{as}}(\text{CH}_3)$], 2869 [$\nu_{\text{s}}(\text{CH}_2)$], 1465 [$\delta_{\text{as}}(\text{CH}_3)$], and 1365 cm^{-1} [$\delta_{\text{s}}(\text{CH}_3)$]. Simultaneously, 2 and 1.8 ± 0.2 neopentane molecules per zirconium (the theoretical value is 2) are selectively evolved during grafting of $\text{Zr}(\text{CH}_2\text{tBu})_4$ to give (3) and (4), respectively. The C/Zr ratios of 9.5 for (3) and 9.3 for (4) are consistent with the expected theoretical value (10) for mainly a bipodal bis(neopentyl)zirconium species (85%). This was reinforced by the Zr/N and C/N ratios obtained, which fit the theoretical values. Further proof came from hydrolysis of these materials at room temperature, which gave 1.7 ± 0.2 and 1.6 ± 0.2 neopentane molecules per Zr for (3) and (4), respectively (Table S1 in the Supporting Information).

All of the ^1H NMR spectra of these grafted Zr complexes display a resonance at 4.4 ppm assigned to the protons of the NH moieties.^{74,100} As expected, the proton signals of the neopentyl fragment appear at about 1 ppm (Figure 5a,b).¹⁰⁰ The 2D DQ ^1H MAS NMR spectrum of (4) confirms the presence of two adjacent NH protons by the presence of a clear autocorrelation on the 2:1 diagonal centered at around 4.4 ppm in F2 and 8.8 ppm in F1 (Figure 5d). This autocorrelation is not present in the 2D spectrum of (3) (Figure 5c), as expected

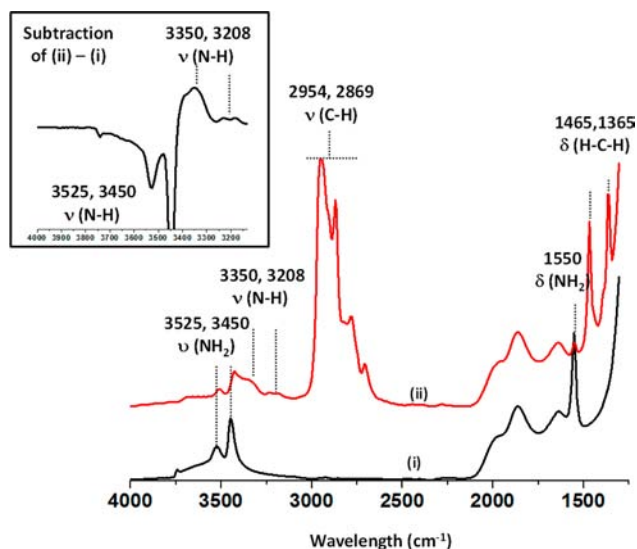


Figure 4. IR spectra of (2) (i) before and (ii) after reaction with $\text{Zr}(\text{CH}_2t\text{Bu})_4$ to give (4). Inset: difference spectrum [(ii) - (i)] showing the disappearance of the ($\equiv\text{SiNH}_2$) stretch modes (3450 and 3525 cm^{-1}) and appearance of the ($\mu\text{-(NH)Si}\equiv$)($\text{OSi}\equiv$) bending mode.

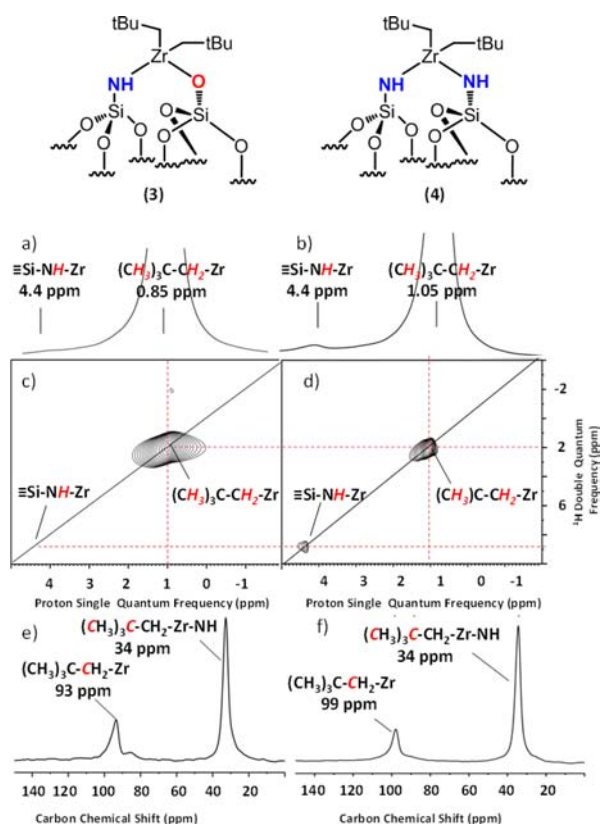


Figure 5. (a, b) ^1H MAS NMR spectra of (3) and (4), respectively. (c, d) DQ rotor-synchronized 2D ^1H MAS spectra of (3) and (4), respectively. (e, f) ^{13}C CP/MAS solid-state NMR spectra of (3) and (4), respectively.

for the generation of a bipodal (silylamido)(silyloxo)bis-(neopentyl)zirconium surface species.

As expected, the autocorrelation for the neopentyl group appears on the 2:1 diagonal centered at around 1 ppm in F2 and 2 ppm in F1. In the ^{13}C NMR spectra (Figure 5e,f), the

signals of the methyl group (from the *t*Bu) appear at 34 ppm for each material. The methylene carbons of the bipodal silylamido/silyloxo complex (3) and the bis-silylamine complex (4) appear at 93 and 99 ppm, respectively. Thus, replacing a nitrogen atom by an oxygen atom induces a slight upfield shift from 99 ppm in (4) to 93 ppm in (3).

Characterizations of Materials (1), (2), (3), and (4). The powder X-ray diffraction patterns of all these materials (Figures S1 and S3 in the Supporting Information) exhibit three clear peaks in the 2θ range of $0.6\text{--}3^\circ$, corresponding to (100), (110), and (200) reflections. They are characteristic of hexagonally ordered mesophases. The structure of each mesoporous material is thus maintained throughout the dehydroxylation followed by ammonia treatment and the $\text{Zr}(\text{CH}_2t\text{Bu})_4$ grafting process.

Nitrogen adsorption–desorption results (Tables S2 and S3 in the Supporting Information) show type-IV isotherms with H1-type hysteresis loops typical of well-ordered mesoporous materials (Figures S2 and S4 in the Supporting Information). After ammonia treatment, the Brunauer–Emmett–Teller (BET) surface area of each material decreases slightly. After reaction with $\text{Zr}(\text{CH}_2t\text{Bu})_4$, the values decrease because of the grafting of large organometallic moieties; however, it should be noted that this grafting does not block the pores of SBA15.

A bright-field transmission electron microscopy (BF-TEM) electron micrograph of the sample of (4) (submitted to the highest ammonia treatment) obtained with high-resolution TEM (HRTEM) confirms the preservation of the hexagonally ordered mesophase (Figure S5A in the Supporting Information), and the results are consistent with those obtained by XRD and nitrogen sorption. All of the elements present in the material were mapped, but here we show the results for Si and Zr. The blue line in the micrograph in Figure S5A shows the position that was used to generate the line profile. The line profile analysis allowed the determination of the widths of the walls and channels in the mesoporous SBA15 (Figure S5B). Typical Si and Zr elemental maps are shown in Figure S5C,D, respectively. Figure S5E shows a trace for the Zr elemental map in Figure S5D. Finally, the Si and Zr maps were superimposed, and the resulting images clearly show the boundaries of the walls and channels in the prepared samples. Figure 6 displays such a superimposed micrograph in which walls (Si-containing areas) are shown in red and channels (Zr-containing areas) are shown in green. The results indicate that Zr was indeed present throughout the channels of the mesoporous silica in a

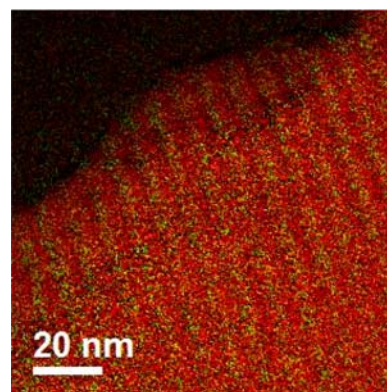
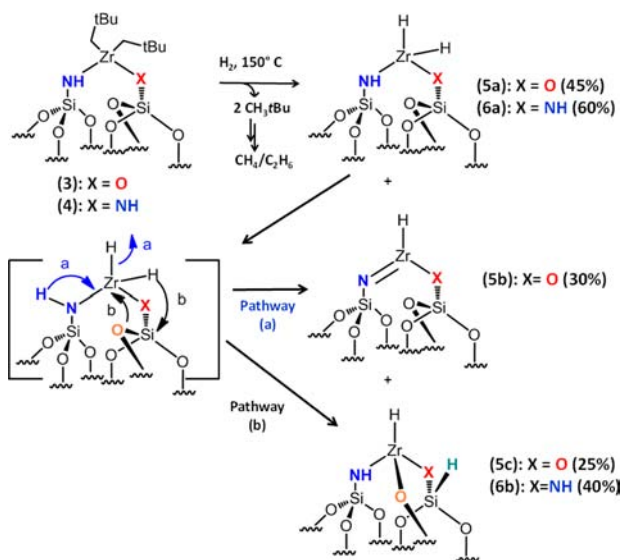


Figure 6. EFTEM image of a sample of (4) (Si and Zr are represented in red and green, respectively).

homogeneous manner. To our knowledge, this is an unprecedented demonstration that the modification of the internal surface of SBA15 by ammonia is homogeneous and that the surface organometallic complexes derived from these ligands are also uniformly distributed inside the pores, despite the size of $\text{Zr}(\text{CH}_2\text{tBu})_4$.

Generation of Supported Zirconium Hydrides. Since two types of silylamido bis(neopentyl)zirconium complexes, (3) and (4), were formed, we used them as precursors of hydrides for possible active sites in the hydrogenolysis of *n*-butane. We expected different behaviors for the hydrides produced from (3) or (4) toward C–H and C–C bond activation and cleavage. Formation of the hydrides required thermal treatment of (3) and (4) at 150 °C for 16 h under H_2 (1 atm) to give (5) and (6). As we will see, we obtained several homologous Zr hydrides (Scheme 3).

Scheme 3. Reactivities of (3) and (4) under H_2 at 150 °C for 16 h



The IR spectra of (3) and (5a, 5b, 5c) and those of (4) and (6a, 6b) are shown in Figures 7 and 8, respectively. The typical vibrational bands of the neopentyl moieties [2954, 2869, 1465, and 1365 cm^{-1} , assigned respectively to $\nu_{\text{as}}(\text{CH}_3)$, $\nu_{\text{s}}(\text{CH}_2)$,

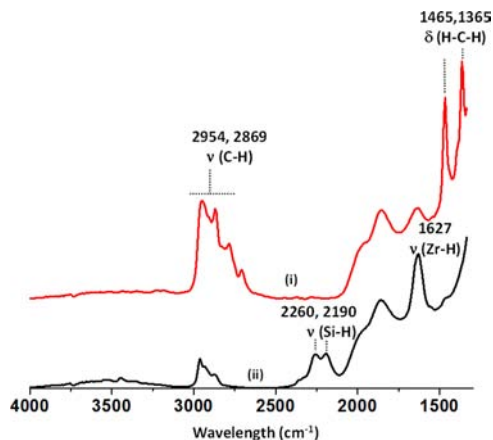


Figure 7. IR spectra of (3) (i) before and (ii) after H_2 (1 atm) treatment at 150 °C for 16 h to give (5).

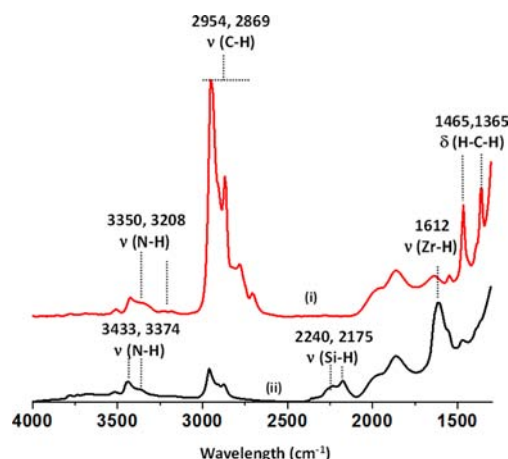
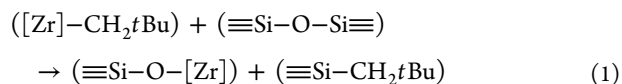


Figure 8. IR spectra of (4) (i) before and (ii) after H_2 (1 atm) treatment at 150 °C for 16 h to give (6).

$\delta_{\text{as}}(\text{CH}_3)$, and $\delta_{\text{s}}(\text{CH}_3)$] almost disappear (reduced by about 90%) after the thermal treatment. In agreement with previous work on silica (Aerosil),^{65,97,101} the formation of zirconium hydride can be highlighted by the presence of a band at 1627 cm^{-1} for (5a, 5b, 5c) and at 1612 cm^{-1} for (6a, 6b). We expected the formation of (silyloxo)(silylamido)zirconium hydride(s) (5) and bis(silylamido)zirconium hydride(s) (6), respectively. During the hydrogenolysis, methane (75%) and ethane (25%) were evolved, corresponding to hydrogenolysis of the two neopentyl fragments formed during the process. Hydrogenolysis also led to the formation of silicon hydride(s) species, characterized by two $\nu(\text{Si-H})$ bands in the 2100 and 2300 cm^{-1} range. According to the literature, the presence of these silicon hydrides is due to the highly oxophilic character of zirconium in zirconium hydride, which reacts with adjacent $\equiv\text{Si-O-Si}\equiv$ bridges, leading to the formation of new $\equiv\text{Si-O-Zr}$ and $\equiv\text{Si-H}$ bonds (Scheme 3).^{65,97} As a result of this process, the $\equiv\text{Si-H}$ group should be in close proximity to the zirconium hydride.

Formation of the new tripodals [$(\equiv\text{Si-NH-})(\equiv\text{Si-O-})_2$]ZrH (5c) and [$(\equiv\text{Si-NH-})_2(\equiv\text{Si-O-})$]ZrH (6b) was confirmed by ^1H NMR spectroscopy (Figure 9). In the DQ ^1H NMR spectrum (Figure 9b) the silicon hydride ($\equiv\text{Si-H}$) correlates with the Zr hydride at 14.7 ppm in the F1 dimension [$\delta_{\text{H}}(\text{Si-H}) + \delta_{\text{H}}(\text{Zr-H}) = 4.5 + 10.2$], confirming the proximity of the $\equiv\text{Si-H}$ and [Zr–H]. While the ^1H NMR spectrum of (6) displays four resonances at 12.1, 10.2, 4.5, and 0.8 ppm (Figure 9c), a fifth signal is observed in the ^1H NMR spectrum of (5) at 14.46 ppm (Figure 9a). This latter has not been previously observed. The intense signal at 0.8 ppm is assigned to the result of alkyl transfers from $\text{Zr}(\text{CH}_2\text{tBu})$ to silicon atoms of ($\equiv\text{Si-O-Si}\equiv$) bridges, which are present in large quantity in SBA15₁₁₀₀ (eq 1):



As expected, the DQ ^1H NMR spectra (Figure 9b,d) clearly show a through-space correlation between the ($\equiv\text{Si-CH}_2\text{tBu}$) moieties (0.8 ppm in F2, 1.6 ppm in F1) and the silicon hydride ($\equiv\text{Si-H}$) (4.5 ppm in F2, 6.1 ppm in F1).¹⁰¹ The signal at 4.5 ppm is also assigned to the amido (NH) proton. The two downfield signals at 12 and 10 ppm are attributed to two types of zirconium hydrides, the bishydride and the

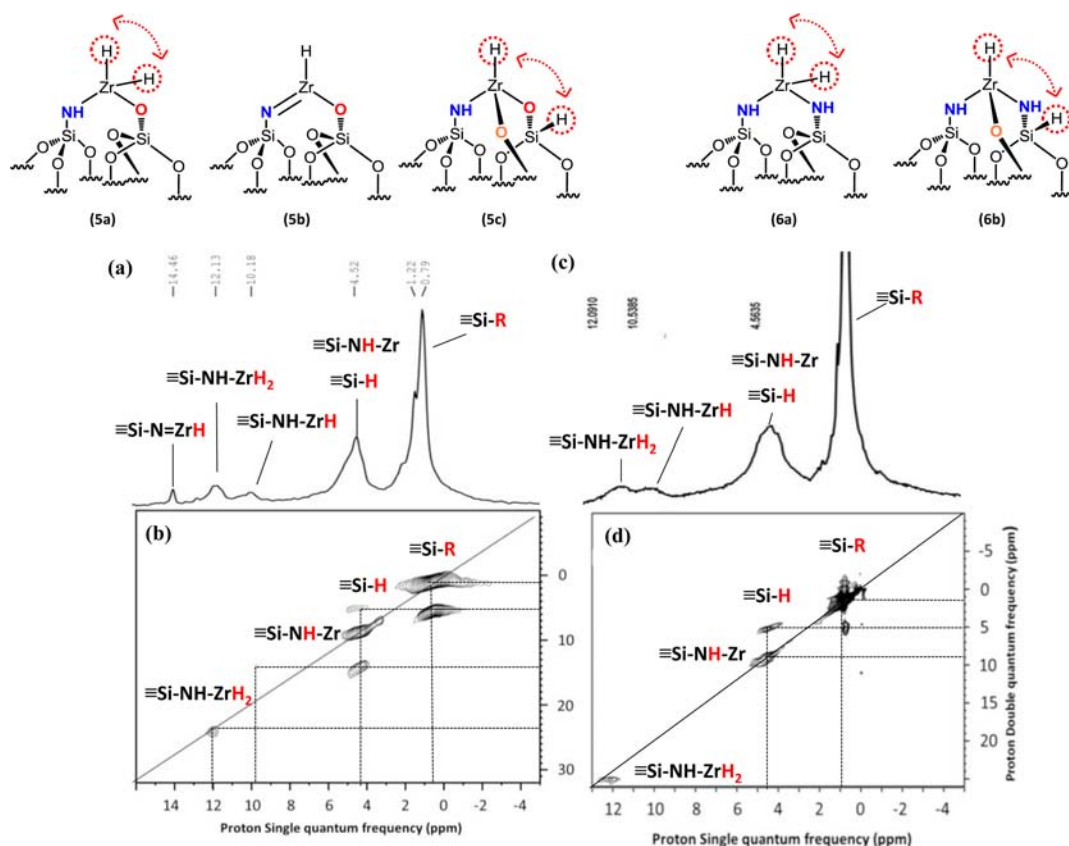


Figure 9. (a) ^1H MAS NMR spectrum of (5). (b) DQ rotor-synchronized 2D ^1H MAS NMR spectrum of [Zr-H] species present on (5). (c) ^1H MAS NMR spectrum of (6). (d) DQ rotor-synchronized 2D ^1H MAS NMR spectrum of [Zr-H] species present on (6).

monohydride (Scheme 3).¹⁰¹ In the 2D spectra in Figure 9b,d, a strong autocorrelation on the diagonal centered at around 12.1 ppm in F2 and 24.2 ppm in F1 is observed: at least two equivalent protons are linked to the same zirconium atom. These observations are in agreement with those obtained in the literature and allow us to assign these signals to the [Zr(H)₂] and [ZrH] species.¹⁰¹

The new resonance at 14.46 ppm can be assigned to a (silylimido)(silyloxo)zirconium hydride, [(≡Si-N=)(≡Si-O-)]ZrH (5b) (Figure 9a). This assignment is reinforced by the DQ ^1H NMR analysis: in the spectrum in Figure 9b, no autocorrelation signal is seen for the proton resonance at 14.46 ppm, indicating that this zirconium hydride group bears only one proton.

To sum up, under H₂ at 150 °C, the material [(≡Si-NH-)(≡Si-O-)]Zr(CH₂tBu)₂ (3) undergoes hydrogenolysis to generate three types of hydride species: [(≡Si-NH-)(≡Si-O-)]Zr(H)₂ (5a), [(≡Si-N=)(≡Si-O-)]ZrH (5b), and [(≡Si-NH-)(≡Si-O-)]₂ZrH (5c) in a 45:30:25 ratio. [(≡Si-NH-)]₂Zr(CH₂tBu)₂ (4) yields the bishydride [(≡Si-NH-)]₂Zr(H)₂ (6a) and the monohydride [(≡Si-NH-)]₂(≡Si-O-)]ZrH (6b) in a 60:40 ratio. Indeed, the bishydride [(≡Si-NH-)]₂Zr(H)₂ (6a) might exist in an elusive resonance structure between two nitrogens of the surface by H₂ elimination, making the characterization of the silylimido species difficult. In the case of the (silylamido)-(silyloxo)zirconium bishydride complex (5a), no resonance structure between the nitrogen and the oxygen is possible. Thus, in other words the [N,O] surface could be considered as an ancillary ligand stabilizing the silylimido species.

Characterization of the Reactivities of the Active Sites in (5) and (6) toward Hydrogenolysis of *n*-Butane.

Electronically unsaturated, neutral four-coordinate zirconium hydrides are important intermediates in the hydrogenolysis of alkanes. Thus, these two highly electrophilic new materials (5) and (6) were also tested in the hydrogenolysis of *n*-butane through C-H activation under mild conditions. The kinetics of the catalytic reactions and the selectivity and conversion of butane versus time for (5) are presented in Figure 10 [the data for (6) are shown in Figure S6 in the Supporting Information]. Both materials were qualitatively active. In each case, the reaction performed efficiently with a typical first-order rate law. Conversion of *n*-butane into lower alkanes first gave a mixture of propane, ethane, and methane with respective selectivities of 22, 55, and 22%, and finally, propane was completely converted into ethane (60%) and methane (40%). Quantitative studies showed that (5) converted 56% of the *n*-butane in 5 h, and total conversion was reached after 16 h. The maximum production of propane was observed after 10 h, which was followed by rapid and a total consumption in 11 h (Figure 10). When the reaction was performed with catalyst (6), the kinetics was much slower (Figure S6). Total conversion of *n*-butane was obtained after 42 h, indicating that (5) is 2.6 times more active than (6). The respective turnover numbers (TONs) at 16 h were 40 and 20. After 5 h, the TON obtained for (5) was 23 and that for (6) was 5; in other words (5) is 4.6 times more active than (6) in this respect (Figure S7 in the Supporting Information).

The key step in this work is that the ammonia treatment leads to mainly (85%) bipodal zirconium complexes on amine-

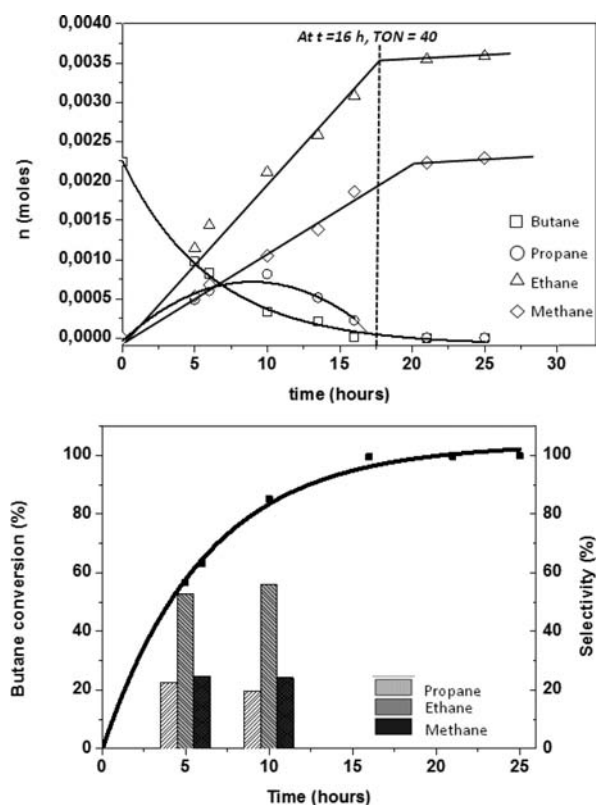


Figure 10. Conversion and selectivity vs time for n -butane (35 Torr) hydrogenolysis (H_2 , 600 Torr) in the presence of (5) at $100^\circ C$ in a batch reactor.

modified SBA15 surfaces (Scheme 2). Following hydrogen treatment, bis-hydride bipodal complexes are the major product. Such results have never been achieved on ordinary highly dehydroxylated silica oxide surfaces (700 – $1000^\circ C$). Indeed, the reaction of $Zr(CH_2tBu)_4$ leads to monopodal complexes $[(\equiv Si-O-Zr(CH_2tBu)_3)]$ that upon hydrogenolysis generate a large amount of tripodal zirconium monohydride $[(\equiv SiO)_3]ZrH$.^{64,101–103} On the basis of all the characterization data and catalytic results, both the presence of the bis-hydride^{66,71} and the combination of nitrogen and oxygen^{33,34} on the surface appear to be essential for enhancement of the catalytic properties of surface organometallic complexes.

CONCLUSION

Well-defined and well-ordered mesoporous silicas containing either silylamine/silanol (1) or bis-silylamine (2) pairs in close proximity have been synthesized by controlled treatment of SBA15₁₁₀₀ with ammonia. These new amine-modified SBA15 surfaces, which were fully characterized by FT-IR and MQ solid-state NMR spectroscopies, were used as a support for novel surface organometallic chemistry exploiting the surface N-donor ligands. Thus, after the reaction with $Zr(CH_2tBu)_4$ on (1) or (2), the results are in accord with bipodal zirconium complexes. The well-defined complexes $[(\equiv Si-NH-)(\equiv Si-O-)]Zr(CH_2tBu)_2$ (3) and $[(\equiv Si-NH-)_2]Zr(CH_2tBu)_2$ (4) lead to the formation of mixtures of new surface hydride complexes [(5) and (6), respectively]. Hydrogenolysis of (5) involves the formation surface hydride complexes (5a), (5b) and (5c). In the case of (6), bis-hydride (6a) and monohydride (6b) coexist on the surface. Both materials (5) and (6) exhibit activities toward C–H and C–C activation and cleavage. Better

activity is observed with (5), certainly due to the presence of the silylamido/silyloxo surface ligands, which allow the formation of an silylimido–silyloxo ancillary ligand. These results highlight the avenues that are opened with these new materials, which offer completely new coordination patterns for surface organometallic chemistry.

EXPERIMENTAL DETAILS

Preparation of SBA15 Dehydroxylated at $1100^\circ C$ (SBA15₁₁₀₀). Typically 2 g of SBA15⁹⁵ was treated in a quartz reactor fitting a tubular furnace under high vacuum (10^{-5} mbar) at $1100^\circ C$ for 16 h. The temperature program was set to $90^\circ C/h$.

$[(\equiv Si-NH-)(\equiv Si-O-)]Zr(CH_2tBu)_2$ (1). SBA-15₁₁₀₀ was placed in a glass tube under a dynamic NH_3 flow at $200^\circ C$ for 30 min. The furnace was cooled to room temperature in a N_2 flow and maintained under dynamic vacuum for 8 h. IR (cm^{-1}): 1550 ($\delta(NH_2)$), 3445 ($\nu_{as}(NH_2)$), 3535 ($\nu_s(NH_2)$). 1H MAS solid-state NMR (400 MHz, $25^\circ C$): δ 0.61 (s, NH_2), 1.73 (s, OH). Elemental analysis (wt %): N, 0.58.

$[(\equiv Si-NH_2)_2]Zr(CH_2tBu)_2$ (2). SBA-15₁₁₀₀ was placed in a glass tube under a dynamic NH_3 flow at $500^\circ C$ for 6 h. The furnace was cooled to room temperature in a N_2 flow and maintained under dynamic vacuum for 8 h. IR (cm^{-1}): 1550 ($\delta(NH_2)$), 3450 ($\nu_{as}(NH_2)$), 3525 ($\nu_s(NH_2)$). 1H MAS solid-state NMR (400 MHz, $25^\circ C$): δ 0.64 (s, NH_2). Elemental analysis (wt %): N, 1.73.

$[(\equiv Si-NH-)(\equiv Si-O-)]Zr(CH_2tBu)_2$ (3). In a double Schlenk tube, (1) (0.5 g) and $Zr(CH_2tBu)_4$ (200 mg, 0.53 mmol) in pentane (20 mL) were stirred at RT over 8 h. The volatiles were then expanded in a 6 L flask, and the beige solid was dried under dynamic vacuum (10^{-5} mbar). IR (cm^{-1}): 1365 ($\delta_s(CH_3)$), 1465 ($\delta_{as}(CH_3)$), 2869 ($\nu_s(CH_2)$), 2954 ($\nu_{as}(CH_3)$), 3208 and 3350 ($\nu(NH)$). 1H MAS solid-state NMR (400 MHz, $25^\circ C$): δ 0.85 (s, CH_2 , CH_3), 4.4 (s, NH). ^{13}C MAS solid-state NMR (400 MHz, $25^\circ C$): δ 34 (s, $C(CH_3)$), 93 (s, CH_2tBu). Elemental analysis (wt %): N, 0.56; C, 5.67; Zr, 4.75.

$[(\equiv Si-NH-)_2]Zr(CH_2tBu)_2$ (4). In a double Schlenk tube, (2) (0.5 g) and $[Zr(CH_2tBu)_4]$ (300 mg, 0.81 mmol) in pentane (25 mL) were stirred at RT over 8 h. The volatiles were then expanded in a 6 L flask, and the beige solid was dried under dynamic vacuum (10^{-5} mbar). IR (cm^{-1}): 1365 ($\delta_s(CH_3)$), 1465 ($\delta_{as}(CH_3)$), 2869 ($\nu_s(CH_2)$), 2954 ($\nu_{as}(CH_3)$), 3208 and 3350 (broad, $\nu(NH)$). 1H MAS solid-state NMR (400 MHz, $25^\circ C$): δ 1.05 (s, CH_2 , CH_3), 4.4 (s, NH). ^{13}C MAS solid-state NMR (400 MHz, $25^\circ C$): δ 34 (s, $C(CH_3)$), 99 (s, CH_2tBu). Elemental analysis (wt %): N, 1.75; C, 8.24; Zr, 6.8.

Reaction of $[(\equiv Si-NH-)(\equiv Si-O-)]Zr(CH_2tBu)_2$ (3) with H_2 To Form Zirconium Hydride Species (5). In a 330 mL reactor, 0.220 g of (3) (0.104 mmol of Zr) was treated with H_2 (1 atm). The temperature was increased to $150^\circ C$ ($1^\circ C/min$) and maintained for 13 h. The color of the solid turned rapidly from beige to gray. IR (cm^{-1}): 1627 ($\nu(Zr-H)$), 2190, 2260 (d, $\nu(Si-H)$), 3358 (broad, $\nu(NH)$). 1H MAS solid-state NMR (400 MHz, $25^\circ C$): δ 0.8 (s, Si–R), 4.52 (s, SiH and NH), 10.2 (s, ZrH , 5c), 12.13 (s, ZrH_2 , 5a), 14.46 (s, $N=ZrH$, 5b). Elemental analysis (wt %): N, 0.56; C, 1.07; Zr, 4.75.

Reaction of $[(\equiv Si-NH-)_2]Zr(CH_2tBu)_2$ (4) with H_2 To Form Zirconium Hydride Species (6). In a 330 mL reactor, 0.280 g of (4) (0.208 mmol of Zr) was treated with H_2 (1 atm). The temperature was increased to $150^\circ C$ ($1^\circ C/min$) and was maintained for 13 h. The color of the solid turned rapidly from beige to gray. IR (cm^{-1}): 1612 ($\nu(Zr-H)$), 2175, 2240 (d, $\nu(Si-H)$), 3375 (broad, $\nu(NH)$). 1H MAS solid-state NMR (400 MHz, $25^\circ C$): δ 0.8 (s, Si–R), 4.56 (s, SiH and NH), 10.5 (s, ZrH , 6b), 12.1 (s, ZrH_2 , 6a). Elemental analysis (wt %): N, 1.73; C, 1.65; Zr, 6.79.

Hydrogenolysis of n -Butane. In a typical reaction, a 330 mL reactor was charged with (5) (110 mg, 4.74 wt % Zr) or (6) (115 mg, 6.79 wt % Zr), n -butane (35 mmHg), and H_2 (1 atm). The reactor was heated to $100^\circ C$. Gases were sampled by opening the reactor to a closed known volume equipped with a septum. The reactor was then reisolated. The known volume was filled to atmospheric pressure with air, and gases were removed by syringe for quantification by GC.

■ ASSOCIATED CONTENT

■ Supporting Information

Detailed experimental procedures, additional data, and Figures S1–S7 and Tables S1–S3. This material is available free of charge via the Internet at <http://pubs.acs.org>.

■ AUTHOR INFORMATION

Corresponding Author

jeanmarie.basset@kaust.edu.sa

Notes

The authors declare no competing financial interest.

■ ACKNOWLEDGMENTS

We gratefully acknowledge the financial support of King Abdullah University of Science and Technology as well as Prof. Kazuhiro Takanabe and Dr. Gregory Biousque for their help in the ammonia treatments and the EFTEM experiments, respectively.

■ REFERENCES

- (1) *Modern Surface Organometallic Chemistry*; Basset, J.-M., Psaro, R., Roberto, D., Ugo, R., Eds.; Wiley-VCH: Weinheim, Germany, 2009.
- (2) Thomas, J. M.; Raja, R.; Lewis, D. W. *Angew. Chem., Int. Ed.* **2005**, *44*, 6456.
- (3) Ternel, J.; Delevoye, L.; Agbossou-Niedercorn, F.; Roisnel, T.; Gauvin, R. M.; Thomas, C. M. *Dalton Trans.* **2010**, 39, 3802.
- (4) Mikhailov, M. N.; Bagatur'yants, A. A.; Kustov, L. M. *Russ. Chem. Bull.* **2003**, *52*, 30.
- (5) Avenier, P.; Taoufik, M.; Lesage, A.; Solans-Monfort, X.; Baudouin, A.; De Mallmann, A.; Veyre, L.; Basset, J.-M.; Eisenstein, O.; Emsley, L.; Quadrelli, E. A. *Science* **2007**, *317*, 1056.
- (6) Chow, C.; Taoufik, M.; Quadrelli, E. A. *Eur. J. Inorg. Chem.* **2011**, 1349.
- (7) Crabb, E. M.; Marshall, R.; Thompsett, D. J. *Electrochem. Soc.* **2000**, *147*, 4440.
- (8) Nichio, N. N.; Casella, M. L.; Santori, G. F.; Ponzi, E. N.; Ferretti, O. A. *Catal. Today* **2000**, *62*, 231.
- (9) Santori, G. F.; Casella, M. L.; Siri, G. J.; Adúriz, H. R.; Ferretti, O. A. *Appl. Catal., A* **2000**, *197*, 141.
- (10) Choi, J.-S.; Maugé, F.; Pichon, C.; Olivier-Fourcade, J.; Jumas, J.-C.; Petit-Clair, C.; Uzio, D. *Appl. Catal., A* **2004**, *267*, 203.
- (11) Marks, T. J. *Acc. Chem. Res.* **1992**, *25*, 57.
- (12) Sautet, P.; Delbecq, F. *Chem. Rev.* **2010**, *110*, 1788.
- (13) Cariati, E.; Recanati, P.; Roberto, D.; Ugo, R. *Organometallics* **1998**, *17*, 1266.
- (14) Lamb, H. H.; Gates, B. C.; Knözinger, H. *Angew. Chem., Int. Ed. Engl.* **1988**, *27*, 1127.
- (15) Zapolko, C.; Liang, Y.; Anwander, R. *Chem. Mater.* **2007**, *19*, 3171.
- (16) Verpoort, F.; Bossuyt, A. R.; Verdonck, L.; Coussens, B. J. *Mol. Catal. A: Chem.* **1997**, *115*, 207.
- (17) Zhizhko, P. A.; Zhizhin, A. A.; Belyakova, O. A.; Zubavichus, Y. V.; Kolyagin, Y. G.; Zarubin, D. N.; Ustynyuk, N. A. *Organometallics* **2013**, *32*, 3611.
- (18) Wolke, S. I.; Buffon, R.; Filho, U. P. R. *J. Organomet. Chem.* **2001**, *625*, 101.
- (19) Lu, J.; Aydin, C.; Browning, N. D.; Gates, B. C. *Langmuir* **2012**, *28*, 12806.
- (20) Ortalan, V.; Uzun, A.; Gates, B. C.; Browning, N. D. *Nat. Nanotechnol.* **2010**, *5*, 506.
- (21) Dufaud, V.; Basset, J.-M. *Angew. Chem., Int. Ed.* **1998**, *37*, 806.
- (22) Lobo-Lapidus, R. J.; Gates, B. C. *J. Catal.* **2009**, *268*, 89.
- (23) Jezequel, M.; Dufaud, V.; Ruiz-Garcia, M. J.; Carrillo-Hermosilla, F.; Neugebauer, U.; Niccolai, G. P.; Lefebvre, F.; Bayard, F.; Corker, J.; Fiddy, S.; Evans, J.; Broyer, J.-P.; Malinge, J.; Basset, J.-M. *J. Am. Chem. Soc.* **2001**, *123*, 3520.
- (24) Dufour, P.; Scott, S. L.; Santini, C. C.; Lefebvre, F.; Basset, J.-M. *Inorg. Chem.* **1994**, *33*, 2509.
- (25) Sankar, G.; Rey, F.; Thomas, J. M.; Greaves, G. N.; Corma, A.; Dobson, B. R.; Dent, A. J. *J. Chem. Soc., Chem. Commun.* **1994**, 2279.
- (26) Maschmeyer, T.; Rey, F.; Sankar, G.; Thomas, J. M. *Nature* **1995**, *378*, 159.
- (27) Pillinger, M.; Nunes, C. D.; Vaz, P. D.; Valente, A. A.; Goncalves, I. S.; Ribeiro-Claro, P. J. A.; Rocha, J.; Carlos, L. D.; Kuhn, F. E. *Phys. Chem. Chem. Phys.* **2002**, *4*, 3098.
- (28) Schrock, R. R. *Acc. Chem. Res.* **1997**, *30*, 9.
- (29) Mountford, P. *Chem. Soc. Rev.* **1998**, *27*, 105.
- (30) Kempe, R. *Angew. Chem., Int. Ed.* **2000**, *39*, 468.
- (31) Roesky, P. W. *Z. Anorg. Allg. Chem.* **2003**, *629*, 1881.
- (32) Schneider, S.; Meiners, J.; Askevold, B. *Eur. J. Inorg. Chem.* **2012**, 412.
- (33) Chong, E.; Qayyum, S.; Schafer, L. L.; Kempe, R. *Organometallics* **2013**, *32*, 1858.
- (34) Lee, A. V.; Schafer, L. L. *Eur. J. Inorg. Chem.* **2007**, 2245.
- (35) Jia, L.; Ding, E.; Rheingold, A. L.; Rhatigan, B. *Organometallics* **2000**, *19*, 963.
- (36) Renner, P.; Galka, C.; Memmler, H.; Kauper, U.; Gade, L. H. J. *Organomet. Chem.* **1999**, *591*, 71.
- (37) Gade, L. H. J. *Organomet. Chem.* **2002**, *661*, 85.
- (38) Schneider, A.; Gade, L. H.; Breuning, M.; Bringmann, G.; Scowen, I. J.; McPartlin, M. *Organometallics* **1998**, *17*, 1643.
- (39) Luo, B.; Kucera, B. E.; Gladfelter, W. L. *Polyhedron* **2006**, *25*, 279.
- (40) Deacon, G. B.; Forsyth, C. M.; Scott, N. M. *Dalton Trans.* **2003**, 3216.
- (41) Kulinna, H.; Spaniol, T. P.; Maron, L.; Okuda, J. *Inorg. Chem.* **2012**, *51*, 12462.
- (42) Lee, L.; Berg, D. J.; Bushnell, G. W. *Organometallics* **1995**, *14*, 8.
- (43) Zhu, X.; Wang, S.; Zhou, S.; Wei, Y.; Zhang, L.; Wang, F.; Feng, Z.; Guo, L.; Mu, X. *Inorg. Chem.* **2012**, *51*, 7134.
- (44) Gauvin, R. M.; Mortreux, A. *Chem. Commun.* **2005**, 1146.
- (45) Revel, B.; Delevoye, L.; Tricot, G.; Rastätter, M.; Kuzdrowska, M.; Roesky, P. W.; Gauvin, R. M. *Eur. J. Inorg. Chem.* **2011**, 1366.
- (46) Gauvin, R. M.; Chenal, T.; Hassan, R. A.; Addad, A.; Mortreux, A. *J. Mol. Catal. A: Chem.* **2006**, *257*, 31.
- (47) Kim, S.-J.; Jung, I. N.; Yoo, B. R.; Cho, S.; Ko, J.; Kim, S. H.; Kang, S. O. *Organometallics* **2001**, *20*, 1501.
- (48) Baumann, R.; Davis, W. M.; Schrock, R. R. *J. Am. Chem. Soc.* **1997**, *119*, 3830.
- (49) Lee, L.; Berg, D. J.; Bushnell, G. W. *Organometallics* **1997**, *16*, 2556.
- (50) Wu, J.-Q.; Pan, L.; Li, Y.-G.; Liu, S.-R.; Li, Y.-S. *Organometallics* **2009**, *28*, 1817.
- (51) Wu, J.-Q.; Mu, J.-S.; Zhang, S.-W.; Li, Y.-S. *J. Polym. Sci., Part A: Polym. Chem.* **2010**, *48*, 1122.
- (52) De Waele, P.; Jazdzewski, B. A.; Klosin, J.; Murray, R. E.; Theriault, C. N.; Vosejka, P. C.; Petersen, J. L. *Organometallics* **2007**, *26*, 3896.
- (53) Liang, L.-C.; Tsai, T.-L.; Li, C.-W.; Hsu, Y.-L.; Lee, T.-Y. *Eur. J. Inorg. Chem.* **2011**, 2948.
- (54) Askevold, B.; Nieto, J. T.; Tussupbayev, S.; Diefenbach, M.; Herdtweck, E.; Holthausen, M. C.; Schneider, S. *Nat. Chem.* **2011**, *3*, 532.
- (55) Tiong, P. J.; Nova, A.; Schwarz, A. D.; Selby, J. D.; Clot, E.; Mountford, P. *Dalton Trans.* **2012**, *41*, 2277.
- (56) Solans-Monfort, X.; Coperet, C.; Eisenstein, O. *J. Am. Chem. Soc.* **2010**, *132*, 7750.
- (57) Bindl, M.; Stade, R.; Heilmann, E. K.; Picot, A.; Goddard, R.; Fürstner, A. *J. Am. Chem. Soc.* **2009**, *131*, 9468.
- (58) Samec, J. S. M.; Grubbs, R. H. *Chem.—Eur. J.* **2008**, *14*, 2686.
- (59) Pietraszuk, C.; Rogalski, S.; Powała, B.; Miętkiewicz, M.; Kubicki, M.; Spólnik, G.; Danikiewicz, W.; Woźniak, K.; Pazio, A.; Szadkowska, A.; Kozłowska, A.; Greła, K. *Chem.—Eur. J.* **2012**, *18*, 6465.

- (60) Kuppaswamy, S.; Ghiviriga, I.; Abboud, K. A.; Veige, A. S. *Organometallics* **2010**, *29*, 6711.
- (61) Liang, L.-C.; Lin, J.-M.; Lee, W.-Y. *Chem. Commun.* **2005**, 2462.
- (62) Wick, D. D.; Goldberg, K. I. *J. Am. Chem. Soc.* **1997**, *119*, 10235.
- (63) Reinartz, S.; White, P. S.; Brookhart, M.; Templeton, J. L. *J. Am. Chem. Soc.* **2001**, *123*, 12724.
- (64) Lecuyer, C.; Quignard, F.; Choplin, A.; Olivier, D.; Basset, J.-M. *Angew. Chem., Int. Ed. Engl.* **1991**, *30*, 1660.
- (65) Lefebvre, F.; Thivolle-Cazat, J.; Dufaud, V.; Niccolai, G. P.; Basset, J.-M. *Appl. Catal., A* **1999**, *182*, 1.
- (66) Besedin, D.; Ustynyuk, L.; Ustynyuk, Y.; Lunin, V. *Top. Catal.* **2005**, *32*, 47.
- (67) Norsic, S.; Larabi, C.; Delgado, M.; Garron, A.; de Mallmann, A.; Santini, C.; Szeto, K. C.; Basset, J.-M.; Taoufik, M. *Catal. Sci. Technol.* **2012**, *2*, 215.
- (68) Niccolai, G. P.; Basset, J.-M. *Appl. Catal., A* **1996**, *146*, 145.
- (69) Rosier, C.; Niccolai, G. P.; Basset, J.-M. *J. Am. Chem. Soc.* **1997**, *119*, 12408.
- (70) Mikhailov, M. N.; Kustov, L. M. *Russ. Chem. Bull.* **2005**, *54*, 300.
- (71) Ustynyuk, L. Y.; Ustynyuk, Y. A.; Laikov, D. N.; Lunin, V. V. *Russ. Chem. Bull.* **2001**, *50*, 2050.
- (72) de With, J.; Horton, A. D. *Angew. Chem., Int. Ed. Engl.* **1993**, *32*, 903.
- (73) De With, J.; Horton, A. D.; Orpen, A. G. *Organometallics* **1990**, *9*, 2207.
- (74) Cummins, C. C.; Baxter, S. M. *J. Am. Chem. Soc.* **1988**, *110*, 8731.
- (75) Cummins, C. C.; Schaller, C. P.; Van Duyne, G. D. *J. Am. Chem. Soc.* **1991**, *113*, 2985.
- (76) Schaller, C. P.; Cummins, C. C.; Wolczanski, P. T. *J. Am. Chem. Soc.* **1996**, *118*, 591.
- (77) Freundlich, J. S.; Schrock, R. R.; Cummins, C. C.; Davis, W. M. *J. Am. Chem. Soc.* **1994**, *116*, 6476.
- (78) Bennett, J. L. *J. Am. Chem. Soc.* **1997**, *119*, 10696.
- (79) Schafer, D. F.; Wolczanski, P. T.; Lobkovsky, E. B. *Organometallics* **2011**, *30*, 6518.
- (80) Schafer, D. F.; Wolczanski, P. T.; Lobkovsky, E. B. *Organometallics* **2011**, *30*, 6539.
- (81) Polse, J. L.; Andersen, R. A.; Bergman, R. G. *J. Am. Chem. Soc.* **1998**, *120*, 13405.
- (82) Blomfield, G. A.; Little, L. H. *Can. J. Chem.* **1973**, *51*, 1771.
- (83) Bendjeriou-Sedjerari, A.; Pelletier, J. D. A.; Abou-hamad, E.; Emsley, L.; Basset, J.-M. *Chem. Commun.* **2012**, *48*, 3067.
- (84) Fink, P.; Muller, B.; Rudakoff, G. J. *Non-Cryst. Solids* **1992**, *145*, 99.
- (85) Yoshida, H.; Inaki, Y.; Kajita, Y.; Ito, K.; Hattori, T. *Stud. Surf. Sci. Catal.* **2002**, *143*, 837.
- (86) Chino, N.; Okubo, T. *Microporous Mesoporous Mater.* **2005**, *87*, 15.
- (87) Wan, K.; Liu, Q.; Zhang, C. *Chem. Lett.* **2003**, *32*, 362.
- (88) Morrow, B. A.; Cody, I. A.; Lee, L. S. M. *J. Phys. Chem.* **1975**, *79*, 2405.
- (89) Morrow, B. A.; Cody, I. A. *J. Phys. Chem.* **1975**, *79*, 761.
- (90) Morrow, B. A.; Cody, I. A. *J. Phys. Chem.* **1976**, *80*, 1998.
- (91) Morrow, B. A.; Cody, I. A.; Lee, L. S. M. *J. Phys. Chem.* **1976**, *80*, 2761.
- (92) Zhao, D.; Feng, J.; Huo, Q.; Melosh, N.; Fredrickson, G. H.; Chmelka, B. F.; Stucky, G. D. *Science* **1998**, *279*, 548.
- (93) Zhao, D.; Huo, Q.; Feng, J.; Chmelka, B. F.; Stucky, G. D. *J. Am. Chem. Soc.* **1998**, *120*, 6024.
- (94) Bunker, B. C.; Haaland, D. M.; Michalske, T. A.; Smith, W. L. *Surf. Sci.* **1989**, *222*, 95.
- (95) Inaki, Y.; Kajita, Y.; Yoshida, H.; Ito, K.; Hattori, T. *Chem. Commun.* **2001**, 2358.
- (96) Puurunen, R. L.; Root, A.; Haukka, S.; Iiskola, E. I.; Lindblad, M.; Krause, A. O. I. *J. Phys. Chem. B* **2000**, *104*, 6599.
- (97) Wang, X.-X.; Veyre, L.; Lefebvre, F.; Patarin, J.; Basset, J.-M. *Microporous Mesoporous Mater.* **2003**, *66*, 169.
- (98) Powell, K. R.; Perez, P. J.; Luan, L.; Feng, S. G.; White, P. S.; Brookhart, M.; Templeton, J. L. *Organometallics* **1994**, *13*, 1851.
- (99) Walsh, P. J.; Hollander, F. J.; Bergman, R. G. *Organometallics* **1993**, *12*, 3705.
- (100) Schaller, C. P.; Cummins, C. C. *J. Am. Chem. Soc.* **1996**, *118*, 591.
- (101) Rataboul, F.; Baudouin, A.; Thieuleux, C.; Veyre, L.; Copéret, C.; Thivolle-Cazat, J.; Basset, J.-M.; Lesage, A.; Emsley, L. *J. Am. Chem. Soc.* **2004**, *126*, 12541.
- (102) Corker, J.; Lefebvre, F.; Lecuyer, C.; Dufaud, V.; Quignard, F.; Choplin, A.; Evans, J.; Basset, J. M. *Science* **1996**, *271*, 966.
- (103) Quignard, F.; Lecuyer, C.; Bougault, C.; Lefebvre, F.; Choplin, A.; Olivier, D.; Basset, J. M. *Inorg. Chem.* **1992**, *31*, 928.